J Membrane Biol (2011) 244:43–53
DOI 10.1007/s00232-011-9396-0

Agonists that Increase $[Ca^{2+}]_i$ Halt the Movement of Acidic Cytoplasmic Vesicles in MDCK Cells

Randi G. Bjaelde · Sigrid S. Arnadottir · Jens Leipziger · Helle A. Praetorius

Received: 3 July 2011 / Accepted: 23 September 2011 / Published online: 12 October 2011

Abstract Translocation of vesicles within the cytoplasm is essential to normal cell function. The vesicles are typically transported along the microtubules to their destination. The aim of this study was to characterize the vesicular movement in resting and stimulated renal epithelial cells. MDCK cells loaded with either quinacrine or acridine orange, dyes taken up by acidic vesicles, were observed at 37°C in semiopen perfusion chambers. Time-lapse series were analyzed by Imaris software. Our data revealed vigorous movement of stained vesicles in resting MDCK cells. These movements seem to require intact microtubules because nocodazole leads to a considerable reduction of the vesicular movements. Interestingly, we found that extracellular ATP caused the vesicular movement to cease. This observation was obvious in time lapse. Similarly, other stimuli known to increase the intracellular Ca^{2+} concentration ($[Ca^{2+}]_i$) in MDCK cells (increment in the fluid flow rate or arginine vasopressin) also reduced the vesicular movement. These findings were quantified by analysis of single vesicular movement patterns. In this way, ATP was found to reduce the lateral displacement of the total population of vesicles by 40%. Because all these perturbations increase $[Ca^{2+}]_i$, we speculated that this increase in $[Ca^{2+}]_i$ was responsible for the vesicle arrest. Therefore, we tested the effect of the Ca^{2+} ionophore, ionomycin (1 μM), which in the presence of extracellular Ca^{2+} resulted in a considerable and sustained reduction of vesicular movement amounting to a 58% decrease in average lateral vesicular displacement. Our data suggest that vesicles transported on microtubules are paused when subjected to high intracellular Ca^{2+} concentrations. This may provide an additional explanation for the cytotoxic effect of high $[Ca^{2+}]_i$.

Keywords Arginine vasopressin · ATP · Ca^{2+} · Flow · MDCK · Vesicle movement

Epithelial cells contain many different types of transport vesicles defined by the donor membrane. They are used in endocytotic and biosynthetic secretory pathways. The endocytotic pathway internalizes extracellular molecules and removes receptors, channels, and transporters from the plasma membrane for recycling or degradation in lysosomes (for review, see Kelly and Owen 2011). On the other hand, the biosynthetic pathway has the capacity to release vesicular content to the exterior or to introduce receptors, channels, or transporters either to the plasma membrane or to specific subcompartments in the cell. Either of the pathways relies on redistribution of the vesicles within the cytoplasm, which requires intact microtubules, kinesins, and dyneins (for review, see Hirokawa 1998). In polarized cells, membrane proteins can be differentially localized to either the apical or basolateral membranes via sorting mechanisms. Basolateral targeting is often determined according to specific primary sequences within the protein, commonly confined to the C-terminal tail of the protein (Casanova et al. 1991; Hunziker et al. 1991; Wolff et al. 2010; Bradley et al. 2010), although N-terminus sequences clearly have been shown to be able to influence the sorting of membrane proteins (Williamson et al. 2008). In many cell types, proteins are not only targeted directly to the

Electronic supplementary material The online version of this article (doi:10.1007/s00232-011-9396-0) contains supplementary material, which is available to authorized users.

R. G. Bjaelde · S. S. Arnadottir · J. Leipziger · H. A. Praetorius (✉)
Department of Biomedicine, Aarhus University, Ole Worms Alle 4, Build. 1160, 8000 Aarhus C, Denmark
e-mail: hp@fi.au.dk

apical or basolateral membrane, but some may also take a detour through the early/recycling endosomal compartment (Farr et al. 2009; Thomas et al. 2004). The early endosomal compartment operates as a dynamic pool for further distribution of membrane and membrane proteins for later fusion with the plasma membrane, secretory vesicles, Golgi apparatus, or lysosomes (Thomas et al. 2004). For apical sorting, many sorting motifs exist, and these often require posttranslational modifications, including glycosylphosphatidylinositol anchored proteins (GPI-AP) (Lisanti et al. 1988, 1989) and proteins containing *N*- or *O*-glycans (Yeaman et al. 1997; Scheiffele et al. 1995). In addition, the recycling endosomal compartment plays a crucial role (for review, see Golachowska et al. 2010).

Molecular motors are generally used for distribution of cytoplasmic elements. Increment in intracellular Ca^{2+} concentration ($[Ca^{2+}]_i$) is known to arrest microtubular-dependent transport of mitochondria in various cell types, including neurons (Rintoul et al. 2003; Chang et al. 2006; Yi et al. 2004). It is of note that the regular axial transport persists even in the presence of very high $[Ca^{2+}]_i$.

Here we report that the vesicular trafficking in a renal epithelial cell line is markedly inhibited by application of various agonists. Our results are consistent with $[Ca^{2+}]_i$ as the primary determining factor because elevation of the $[Ca^{2+}]_i$ in itself is sufficient to halt the vesicular movements. The implication of this finding is that the cellular vesicular redistribution system stops at every stimulation of the cell, which results in an $[Ca^{2+}]_i$ increase. This could imply that overstimulation of the cell by a given agonist potentially modulates the normal homeostasis of the cell.

Methods

Cell Culture

Wild-type MDCK type 1 cells (passages 54–70 from the American Type Culture Collection, Rockville, MD) were grown to confluence on 25-mm-diameter cover slips in Dulbecco modified Eagle medium with 10% fetal bovine serum (Gibco, Invitrogen, Denmark) 2 mM glutamine, 1 U ml^{-1} penicillin, and 100 μg ml^{-1} streptomycin, but without riboflavin as previously described (Praetorius and Spring 2001, 2003). For experiments, we used MDCK cells that have been confluent for at least 4 days. In this state, the MDCK cells show polarization with primary cilia of 4–8 μM apically in the principle cells.

Microscopy and Perfusion

MDCK cell monolayers on coverslips were viewed at 37°C on the stage of an inverted microscope (TE-2000, Nikon) equipped with differential interference contrast combined with low-light-level fluorescence provided via a Xenon lamp and monochromator (Visitech International, Sunderland, UK). Imaging was performed with a long-distance plan Fluo 20×, 0.45 NA or a 60×, 1.4 NA Plan Apo lens (Nikon), an intensified SVGA-charged coupled device (CCD) camera, and imaging software (Quanticell 2000/Image Pro, VisiTech). The cellular fluorescence was sampled at a rate of 1 Hz, and measurements were initiated 60 s before initiation of perfusion. To visualize vesicles just beneath the plasma membrane, we used an imaging setup for total internal reflection fluorescence microscopy. The setup consisted of an IMIC stage (Till-Photonics, Munich, Germany) equipped with three lasers (405 nm Toptica, 488 nm Toptica, and 532 nm Cobolt). A Yanus scan head combined with the Polutrope imaging mode switched the laser beams via a vanometric mirror so that they were concentrated at the back focal plane of the objective. The lasers were adjusted to an angle of ~64° to create an evanescence field around the glass–salt solution interface. The preparation was imaged with a 60×, 1.45 NA Plan Apo (Olympus) objective, and a CCD camera (Sensicam qe, PCO, Kelheim, Germany). The entire setup was delivered from Bio-Science ApS, Gilleleje, Denmark.

The cells were mounted in a semiopen chamber commercially available from Warner Instruments (RC-21BRFS). The chamber was modified to be semiopen, which means that the perfusion chamber is covered by only half a coverslip. In this way, one avoids the building up of pressure in the system and reduces evaporation compared to completely open chambers while retaining the good optical properties of a closed chamber. Solutions were superfused at constant flow rates of 12 μl s^{-1}, which corresponds to a bulk flow velocity of 800 μm s^{-1}.

Measurements of Vesicular Movements

The cells were incubated for 15–30 min with quinacrine (1 μM) or acridine orange (1 μM) at 37°C, and washed twice to remove excess probe. Then they were placed in the perfusion chamber and allowed at least a 20-min period to permit equilibration of the cells at 37°C. Quinacrine was excited at 488 nm and emission was detected above 520 nm; time-lapse image sequences were collected at 1 Hz. The image sequences were thereafter analyzed by Imaris software (Bitplane, Zurich, Switzerland). Analysis of the entire picture in a sequence resulted in too much information for the program to handle. Thus, for every experiment, 4–6 cells were selected in the control period as those showing the highest degree of vesicular movement in this period. This procedure will overestimate the baseline movement for the entire population of cells; however, including cells without initial vesicular movement would

prevent us from estimating the reduction of the movement induced by the various perturbations. The same cells were afterward analyzed on 20 consecutive images, 20 s after initiation of flow (12 μl s^{-1}) or ATP (100 μM). The effect of flow was always investigated in confluent, ciliated cells. In the instance of ionomycin, the vesicular movement was analyzed when the change in $[Ca^{2+}]_i$ was maximal (~100 s after addition of ionomycin, 1 μM). The image sequence was converted to Imaris files, and we used the point tracking option in the software. The same settings were used for all files analyzed. The vesicular size was estimated to be six pixels on background-subtracted images. For estimation of the vesicular position, the option intensity center was chosen and the level adjusted to fit the visible vesicles by eye (the setting was adjusted on the control sequence and used rigorously in the analysis of the flow/agonist treatment). The movement pattern was approximated as Brownian movements through a software option, allowing no more than a 5-pixel jump. The tracks were then filtered for tracks lasting less than 3 s.

Intracellular Ca^{2+} Measurements

The cells were incubated for 30 min with the Ca^{2+}-sensitive probe fluo 4-AM (5 μM) at 37°C and washed twice to remove excess probe. Then they were placed in the perfusion chamber and allowed at least a 20-min de-esterification period. Fluo 4 was excited at 488 nm, and emission was detected above 520 nm. The fluorescence intensity was expressed relative to the baseline value. Changes in $[Ca^{2+}]_i$ were measured in a protocol parallel to the vesicular movement.

Solutions

The perfusion solution had the following composition, in mM: $[Na^+]$ 138, $[K^+]$ 5.3, $[Ca^{2+}]$ 1.8, $[Mg^{2+}]$ 0.8, $[Cl^-]$ 126.9, $[SO_4^{2-}]$ 0.8, HEPES 14, glucose 5.6, probenecid 5, pH 7.4 (37°C, 300 mOsmol l^{-1}). The Ca^{2+}-free solution had the following composition, in mM: $[Na^+]$ 139, $[K^+]$ 5.3, $[Mg^{2+}]$ 0.8, $[Cl^-]$ 125.3, $[SO_4^{2-}]$ 0.8, EGTA 1, HEPES 14, glucose 5.6, probenecid 5, pH 7.4 (37°C, 300 mOsmol). Sources of chemicals were as follows: fluo 4-AM and BAPTA-AM (Invitrogen), probenecid, acridine orange, and quinacrine (Sigma, St. Louis, MO). The solution used in fluo 4 experiments contained 5 mM probenecid to inhibit extrusion of the dye. All experiments were carried out at 37°C, pH 7.4.

Statistical Analysis

All values are provided as mean ± SEM. Statistical significance was determined by the Mann–Whitney–Wilcoxon nonparametric test for comparison of two groups and one-way ANOVA followed by a Tukey–Kramer multiple comparison test for comparison of more than two groups. In both cases, a P value of less than 0.05 was considered significant. The number of observations refers to the number of preparations analyzed.

Results

Quinacrine and Acridine Orange-Labeled Intracellular Vesicles in MDCK Cells

Incubating MDCK cells with either quinacrine or acridine orange resulted in a distinct labeling of cytoplasmic vesicles, with a pattern that was very similar for the two dyes (Fig. 1). Both probes accumulate in acidic vesicles (Palmgren 1991). Acridine orange have been used extensively to study vesicular pH changes (Miedema et al. 1996) and lysosomal exocytosis (Jaiswal et al. 2007). Quinacrine is similarly accumulated in acidic intracellular compartments (Kreda et al. 2007; Marceau et al. 2009). Time-lapse microscopy of MDCK cells stained with these two probes revealed extensive movement of the acidic vesicles within ~70% of the cells, both centrally in the cells and just beneath the plasma membrane (Fig. 2c and Suppl. Movies 1 and 2). The movements of the vesicles can be appreciated as the wavy pattern in the orthogonal views. It should be noted that not all the cells show obvious vesicular movement.

This vesicular movement requires microtubules, as incubation with nocodazole (10 μM) significantly reduced their movement. Figure 2 shows baseline vesicular movements of quinacrine-labeled vesicles of MDCK cells under control conditions (also shown in Suppl. Movie 3A) after 30 min of nocodazole (10 μM, Suppl. Movie 3B) and 30 min after nocodazole is washed out (Suppl. Movie 3C). In the orthogonal views of Fig. 2, one can see the reduction in the movement of the vesicles in the presence of nocodazole; this effect was fully reversible after a 30-min washout period ($n = 5$). The responsiveness of the cells under each condition (control, nocodazole, and washout) was tested in parallel. In these experiments, the changes in fluo 4 fluorescence (as a measure of $[Ca^{2+}]_i$) was measured in response to 100 μM ATP applied apically, and showed a similar response in the absence or presence of nocodazole (10 μM, Fig. 2d).

Increment of Fluid Flow Rate and ATP Freezes Vesicular Movements

Stimulation of P2 receptors on the MDCK cells by ATP (100 μM) caused a striking reduction of the vesicular

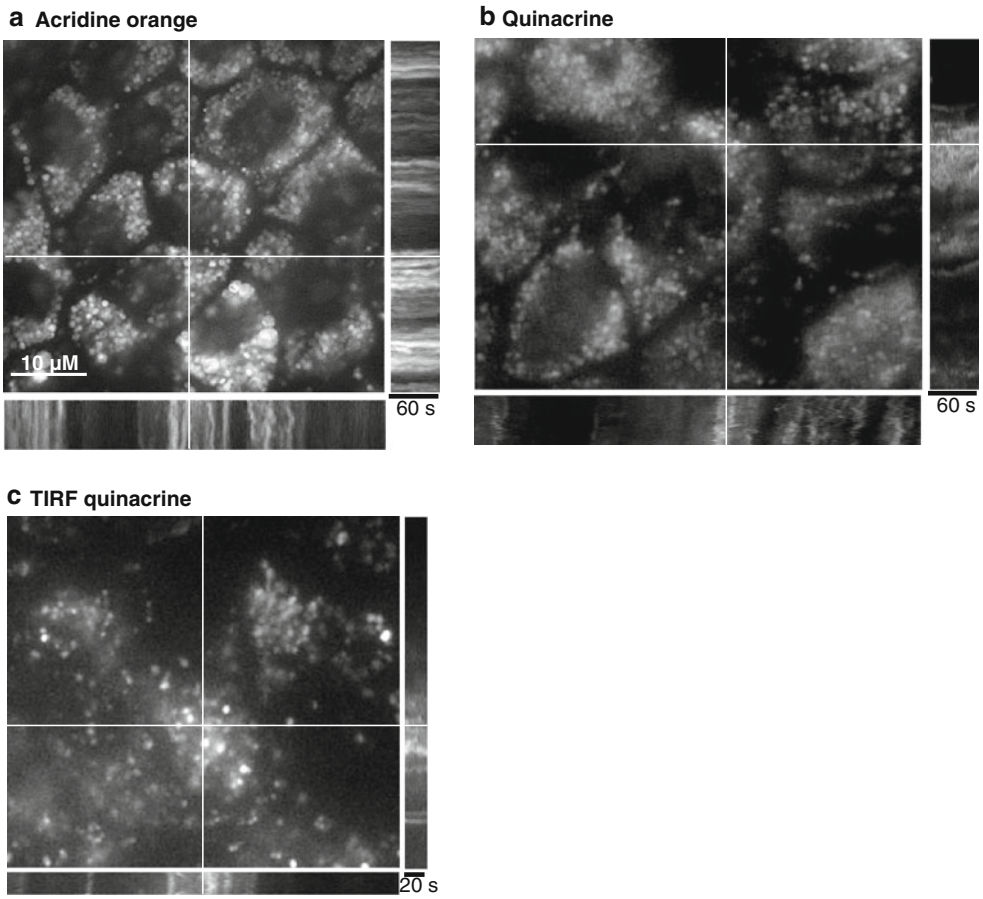

Fig. 1 Vesicular movement in MDCK cells. Time-lapse studies of vesicles labeled with acridine orange (**a**) or quinacrine (**b** and **c**) in MDCK cells at 37°C. The experiments in **c** show vesicles near the plasma membrane captured with total internal reflection fluorescence microscopy. The flickering on the orthogonal views of the image sequence show the vesicular movement in the *line* indicated on the overview image

movement during the application period (Fig. 3 and Suppl. Movie 4). Figure 3a shows experiments conducted in parallel of fluo 4- or quinacrine-loaded MDCK cells. In response to 100 µM ATP, the MDCK cells show the well-described increase in fluo 4 fluorescence, reflecting a rise in the $[Ca^{2+}]_i$. In MDCK cells, the $[Ca^{2+}]_i$ remains elevated from baseline as long as ATP is present (Gordjani et al. 1997). Addition of ATP (100 µM) to the quinacrine-stained MDCK cells revealed that ATP greatly reduced the vesicular movement. This can be seen as a straightening of the lines in the orthogonal views (Fig. 3b), similar to what was observed after incubation with nocodazole. This effect was completely reversible, as the vigorous movements reappeared after washout of ATP. Application of ATP is known to trigger a fast and significant increment in $[Ca^{2+}]_i$. A corresponding ATP-triggered $[Ca^{2+}]_i$ increase is shown in Fig. 3 carried out under parallel conditions to the time lapse of the vesicular movements. Similarly, we could observe that other perturbations known to trigger $[Ca^{2+}]_i$ elevations in MDCK cells also put a brake on the vesicular movements. Increments of the fluid flow rate caused a transient halt of the vesicle movement (Fig. 3d), which in time correlates very well with the transient increase in $[Ca^{2+}]_i$ despite the continuation of the given flow rate (Fig. 3c). Other agonists, such as AVP, which only produce minor increments in $[Ca^{2+}]_i$ (Fig. 3e), and oscillatory activity (Fig. 3f) in MDCK cells also reduced the vesicular movement (Fig. 3g). This may also explain why only a fraction of the cells (~70%) shows vesicular movement. MDCK cells are known to show spontaneous oscillations in $[Ca^{2+}]_i$, which reflect constitutive, unstimulated release of ATP (Geyti et al. 2008), and these underlying oscillations may thus modify the overall vesicular movement.

Quantification of Vesicular Movements

In order to quantify these findings, we used the spot track function in the Imaris software. For every condition, 20 consecutive pictures (sampled at 1 Hz) were analyzed with the exact same settings (see "Methods" section). These results confirm an extensive movement of the vesicles during the control period. This finding is substantiated by the curious bifinding that the total duration of the vesicle tracks was significantly longer during the presence of the agonist (e.g., ATP) compared to control. Going meticulously through the image sequences, this seems to reflect reduced movement in and out of the focal plane during the observation period (16.1 s in the control period and 17.0 s

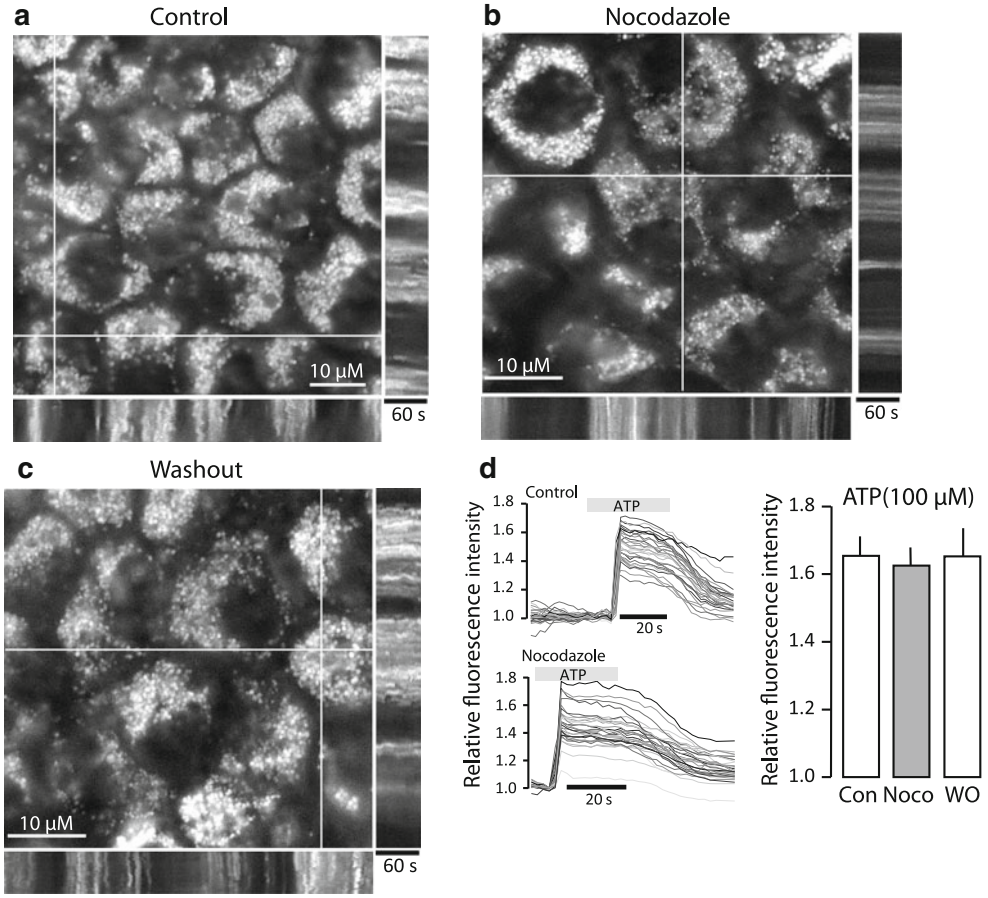

Fig. 2 Effect of nocodazole on vesicular movement in MDCK cells. Time-lapse studies of vesicles labeled with quinacrine (**a**), after 30 min of incubation with nocodazole (10 µM, **b**), and 30 min after washout of nocodazole (**c**). Orthogonal views show the vesicular movement in the *line* indicated on the overview image ($n = 6$). **d** Control experiment for the cells' viability, carried out with the same protocol as the quinacrine-labeled cells. The $[Ca^{2+}]_i$ response to ATP (100 µM) is indicated in the absence and presence of nocodazole (10 µM). *Bars* indicate mean ± SEM; $n = 8$

during application of ATP, $P = 0.0084$). Because of this difference, the single vesicle paths were normalized to the total track duration.

Figure 4a shows all trajectories for the single vesicles identified by the software as the fluorescence intensity peaks. A zoom of the marked area is shown in Fig. 4c. For comparison, Fig. 4b (enhanced area in Fig. 4d) shows what the trajectories look like after addition of ATP (100 µM). It is clear that most vesicles after addition of ATP show less lateral movement and for the main part only show tiny circular movements. This change in pattern is depicted in an alternative way in an *x*–*y* plot in Fig. 4e. Here the track displacement is plotted as a function of track length. This plot shows that many vesicles are reasonably stationary, but few of the total population will show more than 1.5 µm displacement after ATP was added, whereas that is seen quite commonly in the control period. The track length can be considerable even if the lateral movement is small. Figure 4f and g shows the summarized data for all experiments. One can observe a reduction of the lateral displacement by ATP (40.9%) and AVP (29.1%), whereas the increase in fluid flow rate does not show a detectable reduction by the analysis, even though a halt (20–30 s) in the movement is clearly seen by eye when fluid flow rate is increased. This might indicate that the pause in the movement is too brief to be detected in the analysis procedure. For comparison, nocodazole (10 µM for 30 min) reduced the lateral vesicular displacement detected by this analysis procedure by 32.2%. Nevertheless, these findings compelled us to speculate that high $[Ca^{2+}]_i$ directly caused the inhibition of the vesicular movement.

An Increment in Intracellular $[Ca^{2+}]_i$ is Sufficient to Cancel the Vesicular Movements

We investigated the effect of a Ca^{2+} ionophore on the vesicular movements. In exposure to ionomycin (1 µM),

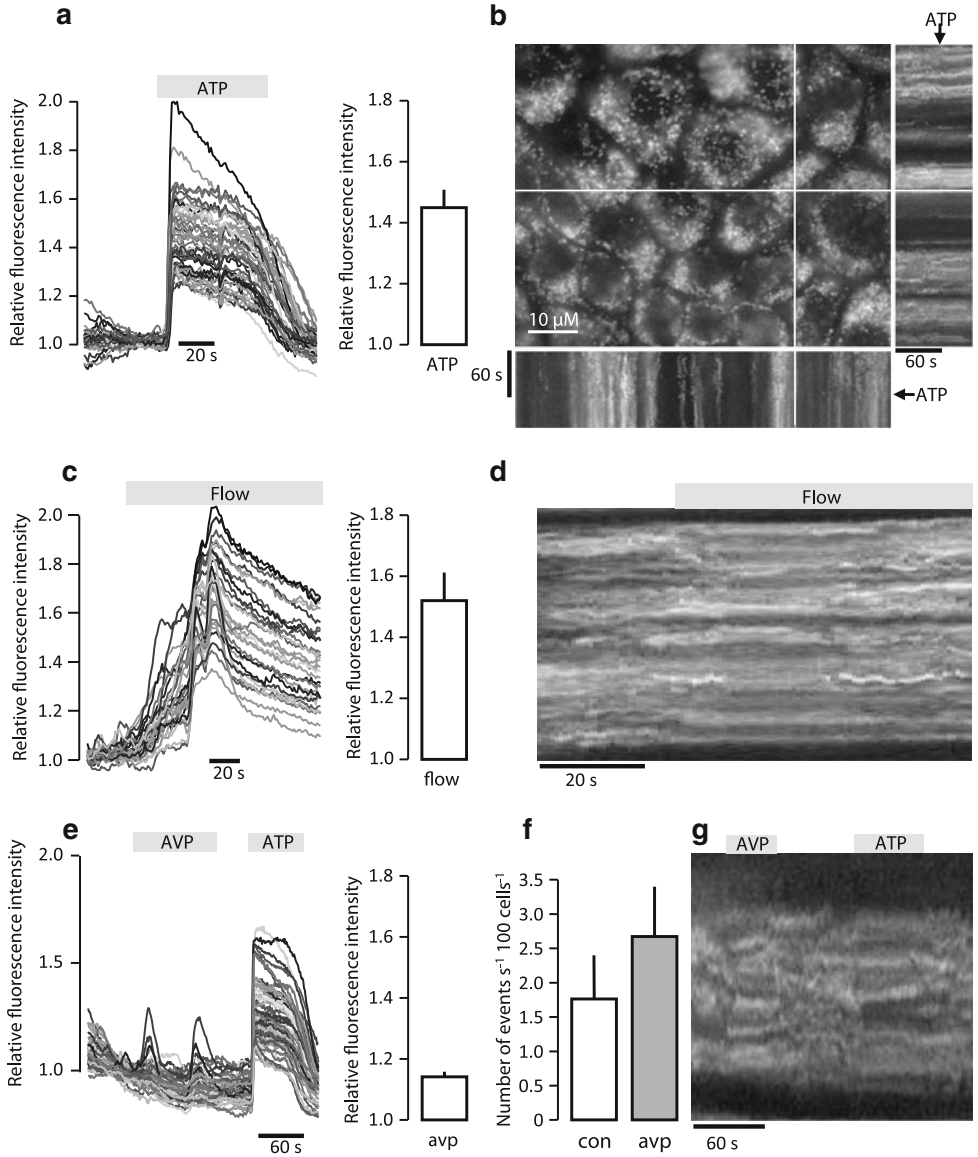

Fig. 3 Stimulation with ATP, AVP, or increment of fluid flow rate reduces vesicular movements. **a**, **b** Effect of ATP on the relative fluo 4 fluorescence and movement of quinacrine-labeled vesicles in living MDCK cells at 37°C. **a** Original trace of the increment in fluo 4 fluorescence of MDCK cells after stimulation with ATP (100 µM); the *bar graph* provides the average amplitude of ATP-induced $[Ca^{2+}]_i$ response ($n = 17$). **b** Orthogonal views show a reduced flickering after exposure to ATP. **c**, **d** Effect of increasing fluid flow rate on the relative fluo 4 fluorescence and the corresponding reduction in vesicular movements. **c** Original trace of the increment in fluo 4 fluorescence of MDCK cells after raising the flow rate from 0 to 12 µl s^{-1}. *Bar graph* provides the average amplitude of flow-induced $[Ca^{2+}]_i$ response ($n = 8$). The reduction in vesicular movement is shown as an orthogonal view. **e–g** Effect of AVP on the relative fluo 4 fluorescence and vesicular movements. **e** Original trace of the increment in fluo 4 fluorescence of MDCK cells after stimulation with AVP (10^{-8} M) followed by ATP (100 µM); *bar graph* shows the average amplitude of AVP-induced $[Ca^{2+}]_i$ response ($n = 16$). **f** *Bar graph* illustrating the number of increments in fluo 4 fluorescence more than 5% over baseline per 100 cells, before and after addition of AVP (10^{-8} M). **g** Orthogonal views show reduced flickering after exposure to AVP and ATP

MDCK cells show a substantial increment in the intracellular Ca^{2+} concentration (Fig. 5). The $[Ca^{2+}]_i$ response is build up slowly to a sustained level, which was maximal after approximately 60 s. Within the same period, the vesicle movements were significantly reduced, both with regard to lateral displacement (58.2%) and track length (29.7%). Similar to the analysis above, the total track duration was longer in the presence of ionomycin compared to control (control 14.2 s, ionomycin with Ca^{2+} 16.1 s, $P = 0.0007$). In the case of ionomycin, the vesicular movement does not resume even after a very long observation period (up to 15 min). This suggests that

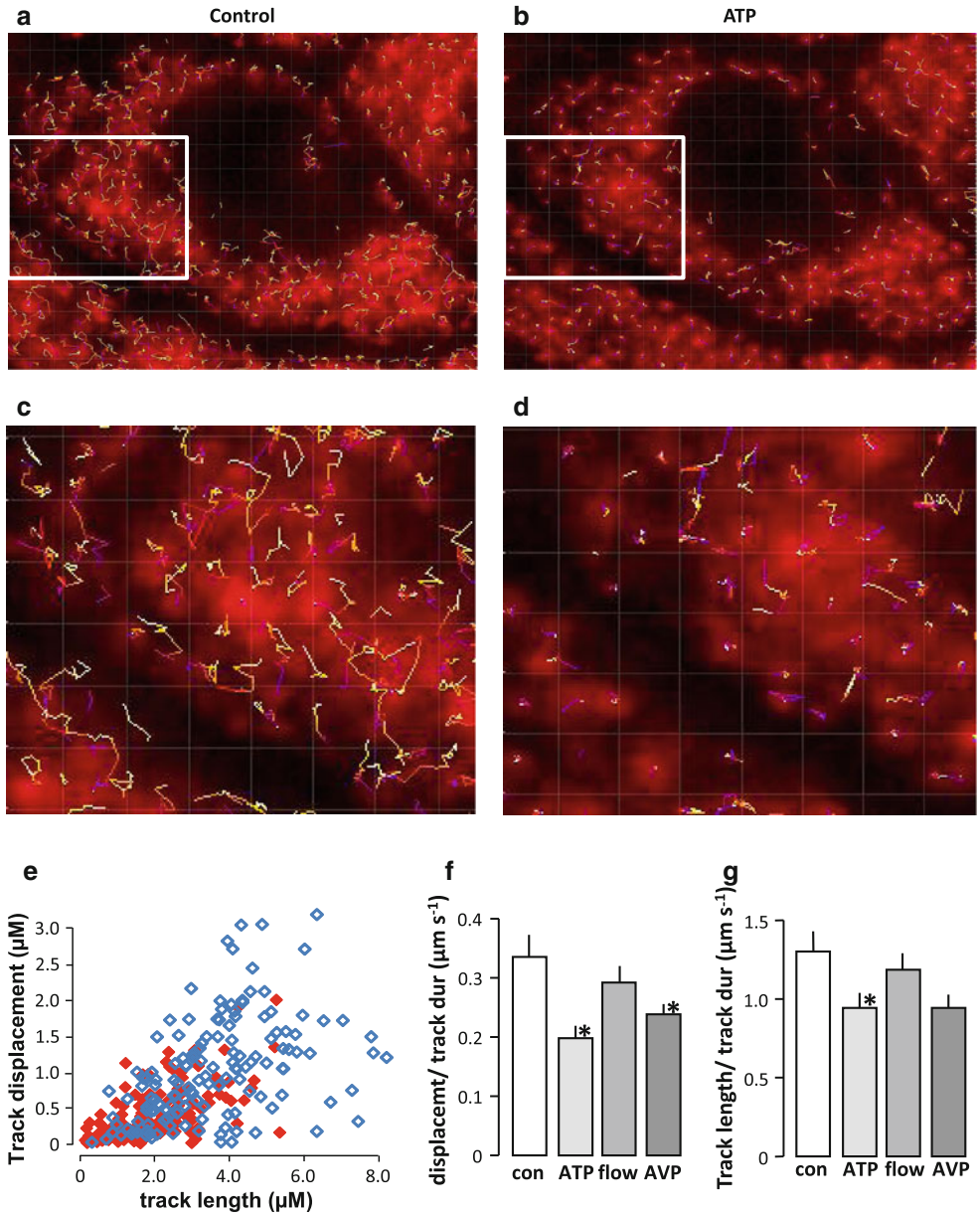

Fig. 4 Analysis of ATP, AVP, or increment of fluid flow-induced reduction of vesicular movement. **a** Spontaneous vesicular movement in the control period. The *lines* reflect the trace for the single vesicles, with a color code starting in the purple area ending in the *yellow–white* area. Vesicular tracking was carried out by Imaris software. **b** Effect of ATP (100 μM) on vesicular displacement. **c**, **d** Close-up of the areas marked by a the *rectangle* in **a** and **b**, respectively. **e** Effect of ATP on vesicular movement shown as a plot of track displacement and track length for the experiment shown above. *Open squares* designate the baseline movement; *closed squares* show the movement after addition of ATP (100 μM). *Bar graphs* indicate full analysis of all experiments for effect on track displacement (**f**) and track length (**g**). Both parameters were normalized for track duration taking into account that vesicles might move in and out of the focal plane during the experiment. *Asterisks* indicates statistically significant reductions ($P < 0.05$); track duration AVP barely reached statistical significance, with $P = 0.0753$ (control $n = 10$, ATP [100 μM] $n = 10$, flow [0–12 μl s^{-1}] $n = 10$, AVP [10^{-8} M], $n = 5$)

increment of $[Ca^{2+}]_i$ levels greatly impair vesicular movement in epithelial cells. If this is the case, one should be able to counteract the effect of agonist and ionophore stimulation by clamping $[Ca^{2+}]_i$ to low values. Loading the MDCK cells with 20 μM BAPTA-AM for 30 min significantly reduced the $[Ca^{2+}]_i$ increments after ATP and ionomycin application (Fig. 5d). When the vesicular movement was analyzed under parallel conditions, it was clear that the lateral displacement of the vesicle was slightly but statistically significantly reduced after application of ATP or ionomycin (by 8.5 and 9.6%, respectively, $P > 0.05$, $n = 8$). In addition, there was no observable effect of ATP and ionomycin on the track length after preincubation with BAPTA-AM.

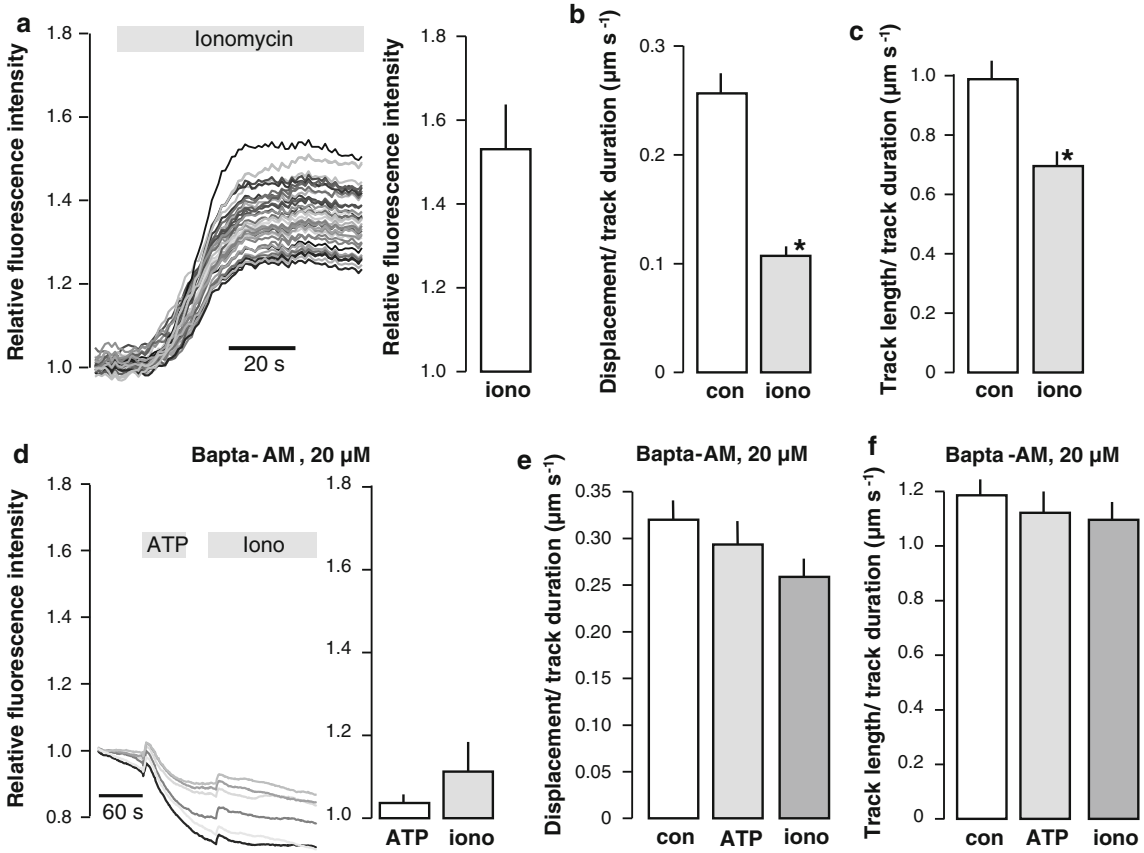

Fig. 5 Effect of ionomycin on vesicular movement in MDCK cells. **a** Original trace of increment in fluo 4 fluorescence in response to ionomycin (1 µM) and summarized data ($n = 9$). **b**, **c** The full analysis of vesicular movement as the track displacement normalized to **b** track duration and **c** the track length. *Asterisks* indicate statistically significant differences, $P < 0.01$ (control $n = 11$, ionomycin with Ca^{2+} $n = 11$). **d** Original trace of the increment in fluo 4 fluorescence in response to ATP (100 µM) and ionomycin (1 µM) of MDCK cells preincubated with BAPTA-AM (20 µM, 30 min, 37°C). **e**, **f** Full analysis of vesicular movement as the track displacement normalized to **e** track duration and **f** the track length in MDCK cells preincubated with BAPTA-AM (20 µM, 30 min, 37°C)

Discussion

MDCK cells (type 1) originate from connecting tubules and collecting ducts of the canine kidney and have been used extensively as an epithelial cell model for polarized membrane trafficking. The epithelial cell model does in culture keep reminiscence of being renal epithelial cells. Even grown on coverslips, the cells readily polarize in the confluent state when allowed to stay as a blend of both intercalated and principle-like cells. This can easily be observed by the formation of primary cilia on the principle-like cells, which normally is over 90% of the cells when cultured, or by a basolateral distribution of the Na^+/K^+ ATPase (Louvard 1980; Caplan et al. 1986). The cells are easy to use in functional assays and do, for example, respond to changes in apical flow rate with a transient increase in $[Ca^{2+}]_i$, a response that requires the primary cilium (Praetorius and Spring 2001, 2003). MDCK cells express numerous receptors through which cellular trafficking can be regulated or modified. One example is ATP/UTP-sensitive P2 receptors (Simmons 1981), which upon activation produce significant increases in the $[Ca^{2+}]_i$ (Gordjani et al. 1997; Zambon et al. 2000; Praetorius et al. 2004; Geyti et al. 2008). Like other polarized cells, they depend on cargo delivery to keep an intact phenotype (Mishra et al. 2010). The cytoplasm of MDCK cells are packed with small vesicles with acidic lumen. These can be visualized in live cell microscopy by loading the cells with the dyes quinacrine and acridine orange. These dyes are taken up and trapped in acidic compartments. In the current study, we have shown that these acidic vesicles readily move around in the cytosol of the MDCK cells. Nocodazole, which inhibits microtubule polymerization, has been shown to reduce the transcytotic and biosynthetic pathway to the apical surface in MDCK cells (Breitfeld et al. 1990). In accordance with this, we found the movement of the acidic vesicles in the MDCK cells to be significantly reduced by preincubation with nocodazole. Cellular organelles are known to be transported along microtubules. This has been thoroughly described for the movement of mitochondria within cells (Stowers et al.

2002; Wang and Schwarz 2009). It was shown that Ca^{2+} is a regulator of kinesin 1's movement of mitochondria. Kinesin heavy chain is constantly associated with the mitochondrion via the mitochondrial protein Miro and the adaptor protein Milton. During high Ca^{2+} concentrations, kinesin heavy chain loses its contact with the microtubules because Ca^{2+} causes the kinesin motor domain to bind to Miro instead of associating with the microtubules (Wang and Schwarz 2009).

The nature of the acidic granules visualized by acridine orange and quinacrine is not addressed in this study. From the low pH in the vesicles, one could assume that it is mainly the lysosomal compartment. Membrane coming from the lysosomal compartment has indeed been shown to fuse with the plasma membrane in, for instance, CHO cells (Thomas et al. 2010), which would imply that this specific compartment would have the need to shift location within the cell. The huge abundance of vesicles seen in the cytosol of the MDCK cells is, however, not consistent with a specific marking of the lysosomes and is likely in addition to the lysosomes to include common endosomes (Wang et al. 2000). This fits very well with the current model for exocytosis in pancreatic acinar cells, where in addition to the well-described release pathway for zymogenic granules is a "minor regulated pathway" for amylase release (Castle et al. 2002), which is stimulated to release via increments in intracellular Ca^{2+}, is bafilomycin dependent, and has an important effect on the overall section (Castle et al. 2002; Weng et al. 2007, 2009; Waterford et al. 2005).

Our result with the applied agonist is consistent with the data for mitochondrial trafficking on microtubules, as the vesicular trafficking is substantially reduced during any perturbation that results in an increase in $[Ca^{2+}]_i$. Mitochondrial transport on the microtubules is abolished at $[Ca^{2+}]_i$ of 1–2 μM (Yi et al. 2004), which is a reasonable concentration range achieved after agonist stimulation in MDCK cells (Vamos et al. 1996). In this context, it should be mentioned that elongation of primary cilia requires intact intraciliary transport. This transport is thoroughly established as a microtubular transport system depending on kinesin II and dynein 1b (for review, see Rosenbaum and Witman 2002), and the elongation is shown to require a strict regulation of the $[Ca^{2+}]_i$ to proceed (Besschetnova et al. 2010). Even though the Ca^{2+} dependency and the effect of nocodazole argue that the vesicular movement observed is primarily mediated by kinesins on microtubules, it by no means disregards the possibility of a contribution of the myosin/actin cytoskeleton. Myosins are, however, generally considered important for tethering of vesicles to active, rich areas of the cell and as modulators of microtubular-dependent transport, rather than being directly involved in actual vesicular movement (for review, see Woolner and Bement 2009).

Our findings underscore the importance of a strict regulation of the $[Ca^{2+}]_i$ for normal vesicular trafficking. Ca^{2+} dependency of vesicular transport has previously been firmly documented in astrocytes, where the directional movement of quinacrine-loaded vesicles is significantly reduced by ionomycin 2 μM (Pangrsic et al. 2007) and is dependent on an intact microtubule cytoskeleton (Potokar et al. 2007). We show that this not only is so for specialized glia, but also that it is equally true in renal epithelial cells. Our findings emphasize that in renal epithelia, the pause in vesicular movement does not require that $[Ca^{2+}]_i$ is clamped at high concentrations for a long time, but is observed at agonist concentrations that result in minor $[Ca^{2+}]_i$ oscillatory elevations. This means that any agonist, even at low concentrations, which cause tiny elevations in $[Ca^{2+}]_i$, greatly reduce the directional vesicular movement in the MDCK cells. The immediate cell biological relevance of this finding is not intuitive and might even seem counterproductive. One could speculate that uncoupling of vesicles from the microtubules is important when the vesicles need to fuse either with other vesicles or with the plasma membrane. The finding is, however, likely to have functional consequences for the cells. One could speculate that prolonged or repeated stimulation with agonists that elevate $[Ca^{2+}]_i$ will impair the normal maintenance of cell function and render the cell more vulnerable to noxious stimuli.

Acknowledgments We thank Edith Bjoern Moeller for technical assistance. We thank the following foundations for their support: the Danish Medical Research Council and the Danish Medical Research Foundation, Nyreforeningens forskningsfond, the Aarhus University Research Foundation, Eva og Henry Frænkels Mindefond, and the A. P. Møller Foundation for the Advancement of Medical Science.

References

Besschetnova TY, Kolpakova-Hart E, Guan Y, Zhou J, Olsen BR, Shah JV (2010) Identification of signaling pathways regulating primary cilium length and flow-mediated adaptation. Curr Biol 20:182–187

Bradley HJ, Liu X, Collins V, Owide J, Goli GR, Smith M, Surprenant A, White SJ, Jiang LH (2010) Identification of an intracellular microdomain of the $P2X_7$ receptor that is crucial in basolateral membrane targeting in epithelial cells. FEBS Lett 584:4740–4744

Breitfeld PP, McKinnon WC, Mostov KE (1990) Effect of nocodazole on vesicular traffic to the apical and basolateral surfaces of polarized MDCK cells. J Cell Biol 111:2365–2373

Caplan MJ, Anderson HC, Palade GE, Jamieson JD (1986) Intracellular sorting and polarized cell surface delivery of (Na^+, K^+)ATPase, an endogenous component of MDCK cell basolateral plasma membranes. Cell 46:623–631

Casanova JE, Apodaca G, Mostov KE (1991) An autonomous signal for basolateral sorting in the cytoplasmic domain of the polymeric immunoglobulin receptor. Cell 66:65–75

Castle AM, Huang AY, Castle JD (2002) The minor regulated pathway, a rapid component of salivary secretion, may provide docking/fusion sites for granule exocytosis at the apical surface of acinar cells. J Cell Sci 115:2963–2973

Chang DT, Honick AS, Reynolds IJ (2006) Mitochondrial trafficking to synapses in cultured primary cortical neurons. J Neurosci 26:7035–7045

Farr GA, Hull M, Mellman I, Caplan MJ (2009) Membrane proteins follow multiple pathways to the basolateral cell surface in polarized epithelial cells. J Cell Biol 186:269–282

Geyti CS, Odgaard E, Overgaard MT, Jensen ME, Leipziger J, Praetorius HA (2008) Slow spontaneous $[Ca^{2+}]_i$ oscillations reflect nucleotide release from renal epithelia. Pflug Arch 455:1105–1117

Golachowska MR, Hoekstra D, van Ijzendoorn SC (2010) Recycling endosomes in apical plasma membrane domain formation and epithelial cell polarity. Trends Cell Biol 20:618–626

Gordjani N, Nitschke R, Greger R, Leipziger J (1997) Capacitative Ca^{2+} entry (CCE) induced by luminal and basolateral ATP in polarised MDCK-C7 cells is restricted to the basolateral membrane. Cell Calcium 22:121–128

Hirokawa N (1998) Kinesin and dynein superfamily proteins and the mechanism of organelle transport. Science 279:519–526

Hunziker W, Harter C, Matter K, Mellman I (1991) Basolateral sorting in MDCK cells requires a distinct cytoplasmic domain determinant. Cell 66:907–920

Jaiswal JK, Fix M, Takano T, Nedergaard M, Simon SM (2007) Resolving vesicle fusion from lysis to monitor calcium-triggered lysosomal exocytosis in astrocytes. Proc Natl Acad Sci USA 104:14151–14156

Kelly BT, Owen DJ (2011) Endocytic sorting of transmembrane protein cargo. Curr Opin Cell Biol 23:404–412

Kreda SM, Okada SF, van Heusden CA, O'Neal W, Gabriel S, Abdullah L, Davis CW, Boucher RC, Lazarowski ER (2007) Coordinated release of nucleotides and mucin from human airway epithelial Calu-3 cells. J Physiol 584:245–259

Lisanti MP, Sargiacomo M, Graeve L, Saltiel AR, Rodriguez-Boulan E (1988) Polarized apical distribution of glycosyl-phosphatidylinositol-anchored proteins in a renal epithelial cell line. Proc Natl Acad Sci USA 85:9557–9561

Lisanti MP, Caras IW, Davitz MA, Rodriguez-Boulan E (1989) A glycophospholipid membrane anchor acts as an apical targeting signal in polarized epithelial cells. J Cell Biol 109:2145–2156

Louvard D (1980) Apical membrane aminopeptidase appears at site of cell–cell contact in cultured kidney epithelial cells. Proc Natl Acad Sci USA 77:4132–4136

Marceau F, Bawolak MT, Bouthillier J, Morissette G (2009) Vacuolar ATPase-mediated cellular concentration and retention of quinacrine: a model for the distribution of lipophilic cationic drugs to autophagic vacuoles. Drug Metab Dispos 37:2271–2274

Miedema H, Staal M, Prins HB (1996) pH-induced proton permeability changes of plasma membrane vesicles. J Membr Biol 152:159–167

Mishra R, Grzybek M, Niki T, Hirashima M, Simons K (2010) Galectin-9 trafficking regulates apical-basal polarity in Madin-Darby canine kidney epithelial cells. Proc Natl Acad Sci USA 107:17633–17638

Palmgren MG (1991) Acridine orange as a probe for measuring pH gradients across membranes: mechanism and limitations. Anal Biochem 192:316–321

Pangrsic T, Potokar M, Stenovec M, Kreft M, Fabbretti E, Nistri A, Pryazhnikov E, Khiroug L, Giniatullin R, Zorec R (2007) Exocytotic release of ATP from cultured astrocytes. J Biol Chem 282:28749–28758

Potokar M, Kreft M, Li L, Daniel AJ, Pangrsic T, Chowdhury HH, Pekny M, Zorec R (2007) Cytoskeleton and vesicle mobility in astrocytes. Traffic 8:12–20

Praetorius HA, Spring KR (2001) Bending the MDCK cell primary cilium increases intracellular calcium. J Membr Biol 184:71–79

Praetorius HA, Spring KR (2003) Removal of the MDCK cell primary cilium abolishes flow sensing. J Membr Biol 191:69–76

Praetorius HA, Frokiaer J, Leipziger J (2004) Transepithelial pressure pulses induce nucleotide release in polarized MDCK cells. Am J Physiol Ren Physiol 288:F133–F141

Rintoul GL, Filiano AJ, Brocard JB, Kress GJ, Reynolds IJ (2003) Glutamate decreases mitochondrial size and movement in primary forebrain neurons. J Neurosci 23:7881–7888

Rosenbaum JL, Witman GB (2002) Intraflagellar transport. Nat Rev Mol Cell Biol 3:813–825

Scheiffele P, Peranen J, Simons K (1995) *N*-glycans as apical sorting signals in epithelial cells. Nature 378:96–98

Simmons NL (1981) Identification of a purine (P2) receptor linked to ion transport in a cultured renal (MDCK) epithelium. Br J Pharmacol 73:379–384

Stowers RS, Megeath LJ, Gorska-Andrzejak J, Meinertzhagen IA, Schwarz TL (2002) Axonal transport of mitochondria to synapses depends on milton, a novel *Drosophila* protein. Neuron 36:1063–1077

Thomas DD, Weng N, Groblewski GE (2004) Secretagogue-induced translocation of CRHSP-28 within an early apical endosomal compartment in acinar cells. Am J Physiol Gastrointest Liver Physiol 287:G253–G263

Thomas DD, Martin CL, Weng N, Byrne JA, Groblewski GE (2010) Tumor protein D52 expression and Ca^{2+}-dependent phosphorylation modulates lysosomal membrane protein trafficking to the plasma membrane. Am J Physiol Cell Physiol 298:C725–C739

Vamos S, Welling LW, Wiegmann TB (1996) Fluorescent analysis in polarized MDCK cell monolayers: intracellular pH and calcium interactions after apical and basolateral stimulation with arginine vasopressin. Cell Calcium 19:307–314

Wang X, Schwarz TL (2009) The mechanism of Ca^{2+}-dependent regulation of kinesin-mediated mitochondrial motility. Cell 136:163–174

Wang E, Brown PS, Aroeti B, Chapin SJ, Mostov KE, Dunn KW (2000) Apical and basolateral endocytic pathways of MDCK cells meet in acidic common endosomes distinct from a nearly-neutral apical recycling endosome. Traffic 1:480–493

Waterford SD, Kolodecik TR, Thrower EC, Gorelick FS (2005) Vacuolar ATPase regulates zymogen activation in pancreatic acini. J Biol Chem 280:5430–5434

Weng N, Thomas DD, Groblewski GE (2007) Pancreatic acinar cells express vesicle-associated membrane protein 2- and 8-specific populations of zymogen granules with distinct and overlapping roles in secretion. J Biol Chem 282:9635–9645

Weng N, Baumler MD, Thomas DD, Falkowski MA, Swayne LA, Braun JE, Groblewski GE (2009) Functional role of J domain of cysteine string protein in Ca^{2+}-dependent secretion from acinar cells. Am J Physiol Gastrointest Liver Physiol 296:G1030–G1039

Williamson RC, Brown AC, Mawby WJ, Toye AM (2008) Human kidney anion exchanger 1 localisation in MDCK cells is controlled by the phosphorylation status of two critical tyrosines. J Cell Sci 121:3422–3432

Wolff SC, Qi AD, Harden TK, Nicholas RA (2010) Charged residues in the C-terminus of the $P2Y_1$ receptor constitute a basolateral-sorting signal. J Cell Sci 123:2512–2520

Woolner S, Bement WM (2009) Unconventional myosins acting unconventionally. Trends Cell Biol 19:245–252

Yeaman C, Le Gall AH, Baldwin AN, Monlauzeur L, Le BA, Rodriguez-Boulan E (1997) The O-glycosylated stalk domain is

required for apical sorting of neurotrophin receptors in polarized MDCK cells. J Cell Biol 139:929–940

Yi M, Weaver D, Hajnoczky G (2004) Control of mitochondrial motility and distribution by the calcium signal: a homeostatic circuit. J Cell Biol 167:661–672

Zambon AC, Hughes RJ, Meszaros JG, Wu JJ, Torres B, Brunton LL, Insel PA (2000) $P2Y_2$ receptor of MDCK cells: cloning, expression, and cell-specific signaling. Am J Physiol Ren Physiol 279:F1045–F1052